Singlet molecular oxygen regulates vascular tone and blood pressure in inflammation

Authors: Christopher P. Stanley[1†], Ghassan J. Maghzal[1,2†], Anita Ayer[1,2], Jihan Talib[1,2], Andrew M. Giltrap[3], Sudhir Shengule[1], Kathryn Wohlhuter[1], Yutang Wang[4¶], Preet Chadha[1], Cacang Suarna[1], Oleksandra Prysyazhna[5], Jenna Scotcher[5], Louise L. Dunn[1,2], Fernanda M. Prado[6], Nghi Nguyen[7], Jephthah O. Odiba[7], Jonathan B. Baell[7,8], Johannes-Peter Stasch[9], Yorihiro Yamamoto[10], Paolo Di Mascio[6], Philip Eaton[5], Richard J. Payne[3] and Roland Stocker[1,2*]

[1]Victor Chang Cardiac Research Institute, Darlinghurst, NSW 2010, Australia

[2]St Vincent's Clinical School, University of New South Wales, NSW 2052, Sydney, Australia

[3]School of Chemistry, The University of Sydney, Sydney, NSW 2006 Australia

[4]Centre for Vascular Research, School of Medical Sciences (Pathology), and Bosch Institute, Sydney Medical School, The University of Sydney, Sydney, NSW 2006, Australia

[5]Department of Cardiology, Cardiovascular Division, King's College London, and The Rayne Institute, St. Thomas' Hospital, London SE1 7EH, UK

[6]Departamento de Bioquímica, Instituto de Química, Universidade de São Paulo, São Paulo, Brazil

[7]Medicinal Chemistry, Monash Institute of Pharmaceutical Sciences, Monash University, Parkville, Victoria 3052, Australia

[8]School of Pharmaceutical Sciences, Nanjing Tech University, No. 30 South Puzhu Road, Nanjing 211816, People's Republic of China

[9]Cardiovascular Research, Bayer AG, Wuppertal, Germany

[10]School of Bioscience and Biotechnology, Tokyo University of Technology, Tokyo, Japan

[†]These authors contributed equally to this manuscript

[¶]Present address: School of Health and Life Sciences, Federation University Australia, Ballarat, VIC 3350, Australia

*Correspondence to: r.stocker@victorchang.edu.au

Singlet molecular oxygen ($^1O_2$) has well-established roles in photosynthetic plants, bacteria and fungi[1-3], but not in mammals. Chemically generated $^1O_2$ oxidizes the amino acid tryptophan to precursors of a key metabolite called *N*-formylkynurenine[4], while enzymatic oxidation of tryptophan to *N*-formylkynurenine is catalyzed by a family of dioxygenases, including indoleamine 2,3-dioxygenase 1[5]. Under inflammatory conditions, this heme-containing enzyme becomes expressed in arterial endothelial cells, where it contributes to the regulation of blood pressure[6]. However, whether indoleamine 2,3-dioxygenase 1 forms $^1O_2$ and whether this contributes to blood pressure control is unknown. Here we show that arterial indoleamine 2,3-dioxygenase 1 regulates blood pressure via formation of $^1O_2$. We observed that in the presence of hydrogen peroxide, the enzyme generates $^1O_2$ and that this is associated with the stereoselective oxidation of L-tryptophan to a tricyclic hydroperoxide via a previously unrecognized oxidative activation of the dioxygenase activity. The tryptophan-derived hydroperoxide acts as a hitherto undiscovered signaling molecule *in vivo*, which induces arterial relaxation and decreases blood pressure dependent on cysteine residue 42 of protein kinase G1α. Our findings demonstrate a pathophysiological role for $^1O_2$ in mammals through formation of an amino acid-derived hydroperoxide that regulates vascular tone and blood pressure under inflammatory conditions.

Several small molecules, such as nitric oxide and hydrogen peroxide (H_2O_2) regulate cellular signaling via interaction with proteins containing redox active metals and/or cysteine residues. Of these molecules, nitric oxide, formed from L-arginine by endothelial nitric oxide synthase, is an important regulator of vascular tone[7]. Sustained increases in nitric oxide synthesis by inducible nitric oxide synthase, as observed in pathological settings such as sepsis, are associated with profound hypotension[8]. Paradoxically, inhibitors of the nitric oxide pathway have generally failed to ameliorate severe septic shock[9,10], suggesting involvement of additional mediators of hypotension.

Based on functional similarity with the metabolism of L-arginine by nitric oxide synthase, we

reported previously that metabolism of L-tryptophan (Trp) to *N*-formylkynurenine (NFK) and kynurenine by endothelial indoleamine 2,3-dioxygenase 1 (IDO1) (Fig. 1a) contributes to the regulation of vascular tone and blood pressure in inflammation[6]. We also showed that commercial kynurenine relaxed pre-constricted arteries, which suggested that kynurenine is an endothelium-derived relaxant factor[6]. Although others have since confirmed these findings[11,12], we noticed that recently purchased kynurenine no longer caused arterial relaxation, and that HPLC-purified kynurenine and NFK also failed to relax naïve mouse arteries (Fig. 1b). However, purified Trp relaxed pre-constricted mouse abdominal aortas that expressed IDO1, irrespective of whether IDO1 expression was induced *in vitro* by treating arteries with interferon-γ or *in vivo* by treating mice with lipopolysaccharide[6] (Fig. 1c, d). These findings indicated that the 'relaxing factor' derived from Trp is likely a biosynthetic metabolite 'upstream' of NFK and that earlier commercial preparations of kynurenine might have contained this molecule as a contaminant.

As chemical oxidation of Trp by $^1O_2$ yields products that decay to NFK[4], and commercial kynurenine can be produced via Trp oxidation by $^1O_2$[13], we exposed Trp to $^1O_2$ *in vitro*. Such '$^1O_2$-exposed Trp' dose-dependently relaxed endothelium-denuded naïve abdominal aortas that do not express IDO1 (Fig. 1e). HPLC/UV analysis revealed '$^1O_2$-exposed Trp' to contain eight distinct compounds (labeled Peaks 1-8, Fig. 1f). By comparison to authentic standards, Peaks 7 and 8 were identified as NFK and Trp, respectively. Of the remaining six individually purified peaks, only Peak 6 was able to substantially relax naïve arteries in a dose-dependent manner (Fig. 1g, Extended data, fig. 1a). Purified Peak 6 also dose-dependently relaxed conduit and resistance arteries from mouse, rat and pig (Extended data, fig. 1b-f), indicating that $^1O_2$-mediated oxidation of Trp generates a compound that relaxes arteries in a vascular bed- and species-independent manner.

We next focused on the chemical identification of the compound eluting in Peak 6. Liquid chromatography mass spectrometry (LC-MS) analysis of '$^1O_2$-exposed Trp' showed that the compounds eluting in Peaks 5 and 6 had a molecular weight of 237 (single ions with m/z 237), and the compounds that eluted in Peaks 2 and 4 had a molecular weight of 221 (Extended data, fig. 2a).

This suggests the incorporation of two and one oxygen atom(s) into Trp (m/z 205), respectively. The MS/MS fragmentation spectra (Extended data, fig. 2b) indicated the compounds of Peaks 2 and 4, and Peaks 5 and 6 to be isomers of each other. Subsequent analysis by ^{1}H and ^{13}C nuclear magnetic resonance (NMR) suggested that the molecules that eluted in Peaks 5 and 6 in the HPLC are tricyclic Trp-derived hydroperoxides with O_2 incorporated at carbon 3a[4], whereas the molecules that eluted in Peaks 2 and 4 are the corresponding tricyclic hydroxides (*trans*- and *cis*-WOH, respectively) with a single oxygen atom incorporated at carbon 3a (Extended data, table 1). We confirmed Peaks 5 and 6 as hydroperoxides by HPLC with post-column chemiluminescence detection[14] (Extended data, fig. 3a). Chemical reduction of purified Peaks 5 and 6 eliminated their chemiluminescence response (Extended data, fig. 3b) and resulted in retention times, molecular ions and fragmentation patterns, and ^{1}H NMR spectra identical to those of Peaks 2 and 4, respectively (Extended data, figs. 3c-d). This data confirmed that Peaks 2 and 4 are the hydroxides of the corresponding hydroperoxides, Peaks 5 and 6, respectively.

To unequivocally assign the stereochemistry of the molecules that eluted in Peaks 5 and 6, we performed Nuclear Overhauser Effect (NOE)-difference NMR on the corresponding stable hydroxide derivatives, Peaks 2 and 4. Irradiation of the resonance at ~5.2 ppm, corresponding to proton H_{8a} in the ^{1}H NMR of purified Peaks 2 and 4, resulted in a clear NOE signal with the α-hydrogen (H_2) in the case of Peak 2 but not Peak 4 (Extended data, figs. 4a-d). Observation of a NOE signal is indicative of protons H_{8a} and H_2 being on the same face of the molecule, which provides information about the relative stereochemistry and suggests that Peak 2 corresponds to the *trans*-configured tricyclic hydroxide. From these findings, extensive 2D NMR analyses, and comparison of the NMR data with relevant literature[4,15], we concluded that the molecule eluting in Peak 6 is the tricyclic Trp-derived *cis*-hydroperoxide ((2*S*,3a*R*,8a*R*)-3a-hydroperoxy-1,2,3,3a,8,8a-hexahydropyrrolo[2,3-b]indole-2-carboxylic acid) (Fig. 1h), hereafter referred to as *cis*-WOOH, while the molecule that eluted in Peak 5 is the corresponding 3a, 8a-epimer *trans*-WOOH (Fig. 1a), in which both positions 3a and 8a are inverted with respect to *cis*-WOOH. Incubation of *cis*-WOOH

at 37 °C and pH 7.4 led to its stoichiometric conversion to NFK, as examined by spectrophotometry, NMR and LC-MS/MS (Extended data, figs. 5a-c), thus establishing *cis*-WOOH as a precursor of NFK. Thermal decomposition of *cis*-WOOH also led to emission of light with maxima at 489 nm, characteristic of activated carbonyls[16] (Extended data, fig. 5d). Based on these findings and known chemistry[4], a plausible scheme for $^1O_2$-mediated conversion of Trp to *cis*-WOOH and its decay to NFK can be proposed (Extended data, fig. 5e).

IDO1 is known as a reductively activated dioxygenase, requiring reduction of its Fe^{3+}-heme prosthetic group to Fe^{2+}-heme for activity[17]. To investigate the potential conversion of Trp to *cis*-WOOH by recombinant human IDO1, we first used superoxide radical anion ($O_2^{\bullet-}$) as a reductant[18] in the presence of Trp and catalase. This resulted in the formation of NFK (Fig. 2a, top) and small amounts of *cis*-WOH, but not *cis*-WOOH. The observed formation of *cis*-WOH supports the previously reported conversion of Trp to a tricyclic hydroxide by reductively activated IDO1[19]. Using cytochrome b_5/cytochrome P450 reductase as a reducing system[20] also yielded NFK and *cis*-WOH but not *cis*-WOOH (Fig. 2a, middle), demonstrating that *cis*-WOOH is not a product of reductively activated dioxygenase activity of IDO1. Because inflammation is associated with increased H_2O_2 and IDO1 also possesses peroxidase activity[21], we next examined Trp oxidation by IDO1 in the presence of H_2O_2. Under these conditions, *cis*-WOOH was formed as the major product, in addition to NFK, the known peroxidase product oxyindolylalanine[22], and trace amounts of *trans*-WOOH (Fig. 2a bottom, Fig. 2b). In contrast, oxidation of Trp with chemically generated $^1O_2$ yielded more comparable amounts of *cis*- and *trans*-WOOH (Fig. 1f, Extended data, figs. 6a-b), indicating that IDO1/H_2O_2 formed *cis*-WOOH as an enzymatic reaction product. Consecutive addition of H_2O_2 at sub-stoichiometric amounts to IDO1 resulted in an H_2O_2 concentration-dependent increase in *cis*-WOOH, with ~0.3 mol of *cis*-WOOH formed per mol of H_2O_2 (Fig. 2b). Pharmacological inhibitors of IDO1 decreased IDO1/H_2O_2-mediated formation of *cis*-WOOH, with the L-isomer of 1-methyltryptophan (1-MT) being more effective than the D-isomer, and with epacadostat and NLG919 (*i.e.*, IDO1 inhibitors of interests as potential anti-cancer adjunct

therapies[23]) being more effective than 1-MT (Extended data, fig. 6c).

Further mechanistic studies revealed that *cis*-WOOH is the product of a previously unrecognized *oxidatively* activated dioxygenase activity of IDO1 (Fig. 2c). Thus, replacing $^{16}O_2$ with $^{18}O_2$ increased the m/z of *cis*-WOOH by 4 amu to 241. In contrast, in reactions using $^{16}O_2$ and $H_2{}^{18}O_2$ instead of $H_2{}^{16}O_2$, *cis*-WOOH retained an m/z of 237 (Fig. 2c, bottom), demonstrating that the two oxygen atoms inserted into Trp to form *cis*-WOOH are derived from O_2 rather than H_2O_2. The O_2-dependence of the Trp to *cis*-WOOH conversion was confirmed by a small but significant increase in *cis*-WOOH when the reaction mixture was saturated with O_2, whereas displacing O_2 in the reaction mixture with argon decreased *cis*-WOOH (and NFK) but not oxyindolylalanine (Fig. 2d).

To determine whether *cis*-WOOH is formed *in vivo*, we pretreated porcine coronary arteries with interferon-γ to increase IDO1 expression[6] and to mimic inflammatory conditions. Such treatment increased arterial H_2O_2 (Fig. 2e) and led to the production of *cis*-WOOH (Fig. 2f), the latter detected by the arterial conversion of $^{15}N_2$ Trp to $^{15}N_2$ *cis*-WOOH. Furthermore, addition of catalase conjugated to polyethylene glycol to scavenge arterial H_2O_2 (but not polyethylene glycol alone) significantly attenuated Trp-induced relaxation of interferon-γ-pretreated mouse arteries (Fig. 2g). Together, these data suggest that under inflammatory conditions arteries produce *cis*-WOOH from Trp and that this is involved in Trp-induced arterial relaxation mediated by IDO1 and H_2O_2.

We next investigated whether IDO1 in the presence of H_2O_2 generates $^1O_2$. Addition of H_2O_2 to Singlet Oxygen Sensor Green (SOSG) and IDO1 resulted in an immediate increase in fluorescence that is characteristic of the $^1O_2$-specific SOSG endoperoxide that was absent when IDO1 was replaced with albumin (Fig. 3a). Similarly, IDO1/H_2O_2 converted anthracene-9,10-diyldiethane-2,1-diyl disulfate disodium salt (EAS)[16] to its $^1O_2$-specific endoperoxide, EAS-O_2 (Fig. 3b). Unambiguous evidence for the formation of $^1O_2$ by IDO1/H_2O_2 was obtained using near infrared emission at 1270 nm, which corresponds to the singlet delta state monomolecular light emission decay of $^1O_2$[24]. Addition of active, but not heat-inactivated IDO1, to H_2O_2 concentration-

dependently increased 1270 nm emission (Fig. 3c). Performing the reaction in H_2O rather than D_2O, as well as removing oxygen, prevented $^1O_2$ formation. Similarly, carbon monoxide prevented $^1O_2$ generation (Fig. 3c, Extended data, fig. 6d and e), indicating the requirement of the heme iron of IDO1 for formation of $^1O_2$. By comparison, nitric oxide partially inhibited $^1O_2$ formation (Fig. 3c, Extended data, fig. 6d), consistent with its previously reported reversible inhibition of IDO1 activity[25]. Together, these findings show, for the first time, that reaction of IDO1 with H_2O_2 generates $^1O_2$.

To assess whether IDO1/H_2O_2-derived $^1O_2$ was utilized for *cis*-WOOH formation, we performed the reaction in D_2O to extend the half-life of $^1O_2$[24]. This increased the yield of *cis*-WOOH relative to that of oxyindolylalanine (Fig. 3d), while the structurally diverse $^1O_2$ scavengers L-histidine, SOSG, *cis*-norbixin and urate decreased the *cis*-WOOH yield (Fig. 3e). LC/MS-based quantification of IDO1/H_2O_2-mediated conversion of EAS to EAS endoperoxide revealed comparable amounts of $^1O_2$ and *cis*-WOOH were formed (Fig. 3f), indicating that the $^1O_2$ generated by IDO1/H_2O_2 accounted for most *cis*-WOOH formed. Similarly, the amounts of *cis*-WOOH formed by IDO1/H_2O_2 were comparable to the extent of conversion of urate to its $^1O_2$-specific oxidation product, parabanic acid[26] (Fig. 3g). This is consistent with the near complete prevention of *cis*-WOOH (Fig. 3e) and SOSG fluorescence (Extended data, fig. 6d) by urate and indicates that the end product of purine metabolism in humans efficiently scavenged the $^1O_2$ formed by IDO1/H_2O_2. Together, these results suggest that IDO1/H_2O_2 generate *cis*-WOOH from Trp via $^1O_2$, and that $^1O_2$ is formed in or near the active site of the enzyme rather than being released into the bulk phase. This conclusion is supported by the observation that the presence of Trp blocked the ability of SOSG to react with $^1O_2$ (Fig. 3a) and decreased 1270 nm emission (Fig. 3c).

If $^1O_2$ were required for conversion of Trp to *cis*-WOOH, other enzymes known to form $^1O_2$ in the presence of H_2O_2[27] may also be able to convert Trp to *cis*-WOOH. Indeed, horseradish peroxidase and myeloperoxidase, as well as purified IDO2, formed *cis*-WOOH, albeit with lower stereospecificity than IDO1 (Extended data, fig. 6f). The fact that IDO2, like IDO1, generated *cis*-

WOOH in the presence of H_2O_2 raised the possibility that IDO2 may also contribute to Trp-mediated arterial relaxation under inflammatory conditions. To test this possibility, we compared Trp-induced relaxation of IFNγ-pretreated abdominal aortas of WT, *Ido1*$^{-/-}$ and *Ido1*$^{-/-}$*Ido2*$^{-/-}$ mice. Relaxation was attenuated to a comparable extent in arteries from *Ido1*$^{-/-}$ and *Ido1*$^{-/-}$*Ido2*$^{-/-}$ mice (Extended data, fig. 6g). This indicates that under the conditions tested IDO2 may not play a significant role in arterial relaxation, consistent with a lack of evidence for arterial expression of IDO2 in naïve animals or under conditions of inflammation.

Known mechanisms of $^1O_2$ generation by dark reactions in biochemical systems involve superoxide radical anion, thiyl radicals, hypochlorite plus H_2O_2, energy transfer from excited triplet carbonyls, or peroxyl radicals.[27] In the case of IDO1/H_2O_2, superoxide and thiyl radicals are likely not involved since addition of superoxide dismutase (to scavenge superoxide) or *N*-ethylmaleimide (to block thiols) did not affect *cis*-WOOH formation (Extended data, fig. 7a and b). Any involvement of hypochlorite was excluded based on the absence of conversion of hydroethidine to 2-chloroethidium[28] by IDO1/H_2O_2 (Extended data, fig. 7c). In addition, sorbate, a scavenger of excited carbonyls[16], decreased the yield of *cis*-WOOH formation modestly, whereas the oxygen-centered radical scavenger, 5,5-dimethyl-1-pyrroline *N*-oxide (DMPO) was more effective (Extended data, fig. 7d). The implied involvement of protein peroxyl radicals in the formation of $^1O_2$ by IDO1 was supported by the appearance of IDO1 dimers (upper arrow in Extended data, fig. 7e), IDO1-associated dityrosine-specific fluorescence (Extended data, fig. 7f), and protein hydroperoxides (Extended data, fig. 7g). DMPO effectively inhibited the formation of these species, just as it inhibited IDO1/H_2O_2-mediated conversion of EAS to EAS-O_2 (Extended data, fig. 7h). These findings and previous studies by others[29] suggest that the reaction of IDO1 with H_2O_2 yields a porphyrin radical, which delocalizes to aromatic amino acid residues of IDO1, most likely a Tyr residue. The resulting amino acid-derived phenoxyl radical may then engage in dityrosine formation, β-scission and/or fragmentation reactions, as well as formation of protein peroxyl radicals (Extended data, scheme 1), in accordance with known chemistry[30]. Consistent with this

possibility, reaction of IDO1 with H_2O_2 generated IDO1 fragments (double arrow in Extended data, fig. 7e) and excited carbonyls (Extended data, fig. 7i), both of which were inhibited by Trp and DMPO. Moreover, others reported previously[22] that in the presence H_2O_2 and DMPO, IDO1 generates IDO1-DMPO adducts, indicative of protein radicals[31]. Based on these results, we propose the Russell mechanism[32] as a possible pathway for the formation of $^1O_2$ by IDO1/H_2O_2 (Extended data, scheme 1).

Having established the importance of $^1O_2$ in IDO1/H_2O_2-mediated formation of *cis*-WOOH, we examined the effect of $^1O_2$ scavenging on Trp-induced IDO1-mediated arterial relaxation. Addition of the $^1O_2$ scavengers L-histidine, urate or *cis*-norbixin to interferon-γ-pretreated arteries from wildtype mice significantly attenuated relaxation mediated by Trp but not nitric oxide (Fig. 3h-i, Extended data, fig. 6h), an effect not seen with arteries from *Ido1*$^{-/-}$ mice (Fig. 3h). Moreover, addition of urate to interferon-γ-pretreated arteries resulted in the accumulation of parabanic acid (Fig. 3j). Together, these data indicate that IDO1-expressing arteries form $^1O_2$ under conditions that mimic inflammation.

Having identified *cis*-WOOH as a novel relaxant derived from Trp via IDO1-mediated formation of $^1O_2$, we next focused on the mechanism of *cis*-WOOH-mediated relaxation in resistance arteries. Given the role of protein kinase G (PKG) in arterial relaxation, we focused on this as the initial target of *cis*-WOOH. The cGMP-competitive PKG inhibitor RP-8CPT modestly attenuated *cis*-WOOH-mediated relaxation, whereas the ATP-competitive PKG inhibitor KT5823 was more effective (Extended data, fig. 8a, b), suggesting cGMP-independent activation of PKG by *cis*-WOOH. PKG1α is known to undergo H_2O_2-mediated oxidative dimerization through cysteine residue 42 (C42), which targets the kinase and is associated with its activation[33]. Amino acid hydroperoxides can also oxidize protein thiol residues[34]. Interestingly, we observed that *cis*-WOOH, but not *trans*-WOOH, dimerized purified recombinant human PKG1α (Fig. 4a). *cis*-WOOH-mediated dimerization was independent of the presence of transition metals and light, but dependent on C42 of PKG1α, as the C42S mutant of PKG1α was refractory to dimerization (Fig.

4a). Exposure of resistance arteries of wildtype (Fig. 4b, left) and *Ido1*$^{-/-}$ mice (Fig. 4b, right) to *cis*-WOOH also caused PKG1α dimerization, as was observed with Trp addition to IDO1-expressing arteries (Fig. 4c). Compared with the wildtype counterparts, mesenteric arteries from PKG1α C42S knock-in mice[35] showed blunted relaxation in response to *cis*-WOOH and Trp, but not the nitric oxide donor DEANO (Fig. 4d).

We previously reported that *Ido1*$^{-/-}$ mice are partially protected from hypotension induced by experimental cerebral malaria and endotoxemia[6], and that IDO1 activity increases considerably and predicts the vasopressor needs in patients with severe sepsis[36]. To examine the role of the IDO1/*cis*-WOOH/PKG1α in the regulation of blood pressure in inflammation, we therefore compared systolic blood pressure responses in unconscious endotoxemic wildtype and PKG1α C42S knock-in mice. Infusion of Trp decreased blood pressure temporarily in wildtype but not knock-in mice (Fig. 4e), while IDO activity was comparable between the two genotypes (Extended data, fig. 8d and e). In contrast to Trp, the hypotensive response to sodium nitroprusside, that activates PKG1α via the canonical non-oxidative pathway, was comparable in wildtype and PKG1α C42S knock-in mice (Fig. 4f). These data directly support the notion that the Trp-induced decrease in blood pressure of endotoxemic mice is mediated via non-canonical oxidative activation of PKG1α involving C42.

As H_2O_2 itself can induce arterial relaxation via C42-dependent oxidative dimerization of PKG1α, we asked whether this pathway overlaps with PKG1α oxidation by *cis*-WOOH. To examine this possibility, we tested the effect of Trp on acetylcholine-induced relaxation of resistant mesenteric arteries that is considered to be mediated by H_2O_2.[37] Trp and 1-MT had no material effect on arteries isolated from naïve mice (Fig. 4g), whereas Trp sensitized and 1-MT attenuated the relaxation of arteries from endotoxemic mice (Fig. 4h). Moreover, addition of Trp to IDO1-expressing human vascular smooth muscle cells augmented PKG1α dimerization by 1 μM H_2O_2, a concentration that itself did not induce measurable dimerization (Fig. 4i). These results suggest that under inflammatory conditions, H_2O_2-induced regulation of arterial relaxation via PKG1α oxidation may be partially mediated by IDO1/*cis*-WOOH.

We finally tested the potential role of IDO1/*cis*-WOOH in cardiac pathophysiology related to pressure-overload, where PKG1α oxidation has been implicated[38]. Under the conditions tested, we found no evidence for IDO1 expression and hence role in cardiac tissue after pressure-overload (Extended data, fig. 9a). In contrast, IDO1 was expressed in conduit arteries with underlying atherosclerosis, as well as in resistance vessels of apolipoprotein E gene knockout (*Apoe*$^{-/-}$) but not *Apoe*$^{-/-}$*Ido1*$^{-/-}$ mice. More importantly, IDO1 also contributed to the regulation of blood pressure in *Apoe*$^{-/-}$ but not in *Apoe*$^{-/-}$*Ido1*$^{-/-}$ mice (Extended data, fig. 9b-f), indicating that the pathway identified here may play a role in blood pressure regulation in atherosclerosis, an inflammatory disease.

In summary, we have demonstrated that $^1O_2$ plays an important pathophysiological role in the redox regulation of arterial relaxation and blood pressure in mammals under inflammatory conditions where IDO1 is expressed. While mammalian enzymes such as myeloperoxidase have long been known to be capable of forming $^1O_2$[27], a physiological or pathophysiological role for $^1O_2$ in mammals outside photosensitization reactions has not been established to date. Our findings also suggest an expanded range of biological functions for IDO1, and serve as the starting point for discovery of a refined repertoire of redox signaling paths by H_2O_2. For example, the biological activities uncovered here highlight the IDO1/PKG1α axis as a possible therapeutic target in sepsis, where oxidative activation of PKG1α[39] and IDO1 activity are prevalent[36]. They also raise the possibility that the highly reactive and potentially cytotoxic $^1O_2$[40] may contribute to IDO1-mediated immune tolerance and tumor evasion, with inhibition of IDO1 representing a major target of anti-cancer drug development[41,42]. Our study shifts focus from H_2O_2 to an amino acid-derived hydroperoxide as a stereospecific signaling molecule. Other heme proteins known to generate $^1O_2$ in the presence of H_2O_2[27] may therefore also play key roles in redox signaling by forming products that, like *cis*-WOOH, act as signaling molecules.

References

1 Triantaphylidès, C. & Havaux, M. Singlet oxygen in plants: production, detoxification and signaling. *Trends Plant Sci.* **14**, 219-228 (2009).

2 Glaeser, J., Nuss, A. M., Berghoff, B. A. & Klug, G. Singlet oxygen stress in microorganisms. *Adv. Microb. Physiol.* **58**, 141-173 (2011).

3 Beseli, A., Goulart da Silva, M. & Daub, M. E. The role of *Cercospora zeae-maydis* homologs of *Rhodobacter sphaeroides* $^1O_2$-resistance genes in resistance to the photoactivated toxin cercosporin. *FEMS Microbiol. Lett.* **362**, 1-7 (2015).

4 Ronsein, G. E., Oliveira, M. C., Miyamoto, S., Medeiros, M. H. G. & Di Mascio, P. Tryptophan oxidation by singlet molecular oxygen [$O_2(^1\Delta_g)$]: mechanistic studies using ^{18}O-labeled hydroperoxides, mass spectrometry, and light emission measurements. *Chem. Res. Toxicol.* **21**, 1271-1283 (2008).

5 Efimov, I. *et al.* Structure and reaction mechanism in the heme dioxygenases. *Biochemistry* **50**, 2717-2724 (2011).

6 Wang, Y. *et al.* Kynurenine is an endothelium-derived relaxing factor produced during inflammation. *Nat. Med.* **16**, 279-285 (2010).

7 Ignarro, L. J., Cirino, G., Casini, A. & Napoli, C. Nitric oxide as a signaling molecule in the vascular system: an overview. *J. Cardiovasc. Pharmacol.* **34**, 879-886 (1999).

8 Gomez-Jimenez, J. *et al.* L-arginine: nitric oxide pathway in endotoxemia and human septic shock. *Crit. Care Med.* **23**, 253-258 (1995).

9 López, A. *et al.* Multiple-center, randomized, placebo-controlled, double-blind study of the nitric oxide synthase inhibitor 546C88: effect on survival in patients with septic shock. *Crit. Care Med.* **32**, 21-30 (2004).

10 Bakker, J. *et al.* Administration of the nitric oxide synthase inhibitor N^G-methyl-L-arginine hydrochloride (546C88) by intravenous infusion for up to 72 hours can promote the resolution of shock in patients with severe sepsis: results of a randomized, double-blind, placebo-controlled multicenter study (study no. 144-002). *Crit. Care Med.* **32**, 1-12 (2004).

11 Sakakibara, K. *et al.* Kynurenine causes vasodilation and hypotension induced by activation of KCNQ-encoded voltage-dependent K^+ channels. *J. Pharmacol. Sci.* **129**, 31-37 (2015).

12 Fazio, F. *et al.* Vasorelaxing action of the kynurenine metabolite, xanthurenic acid: the missing link in endotoxin-induced hypotension? *Front. Pharmacol.* **8**, 214 (2017).

13 Sanders, J., Peter, F., Scott, E., Saad, M. H. & Carr, R. H. Process for converting tryptophan into kynurenine. *World Intellectual Property Organization* WO 2009/135843 A1.

14 Yamamoto, Y., Brodsky, M. H., Baker, J. C. & Ames, B. N. Detection and characterization of lipid hydroperoxides at picomole levels by high-performance liquid chromatography. *Anal. Biochem.* **160**, 7-13 (1987).

15 Nakagawa, M. *et al.* Dye-sensitized photooxygenation of tryptophan: 3a-hydroperoxypyrroloindole as a labile precursor of formylkynurenine. *Chem. Pharm. Bull. (Tokyo)* **29**, 1013-1026 (1981).

16 Mano, C. M. *et al.* Excited singlet molecular O_2 ($^1\Delta_g$) is generated enzymatically from excited carbonyls in the dark. *Sci. Rep.* **4**, 5938 (2014).

17 Taniguchi, T. *et al.* Indoleamine 2,3-dioxygenase. Kinetic studies on the binding of superoxide anion and molecular oxygen to the enzyme. *J. Biol. Chem.* **254**, 3288-3294 (1979).

18 Ohnishi, T., Hirata, F. & Hayaishi, O. Indoleamine 2,3-Dioxygenase. Potassium superoxide as substrate. *J. Biol. Chem.* **252**, 4643-4647 (1977).

19 Basran, J. *et al.* The mechanism of formation of *N*-formylkynurenine by heme dioxygenases. *J. Am. Chem. Soc.* **133**, 16251-16257 (2011).

20 Maghzal, G. J., Thomas, S. R., Hunt, N. H. & Stocker, R. Cytochrome b_5, not superoxide anion radical, is a major reductant of indoleamine 2,3-dioxygenase in human cells. *J. Biol. Chem.* **283**, 12014-12025 (2008).

21 Shimizu, T., Nomiyama, S., Hirata, F. & Hayaishi, O. Indoleamine 2,3-dioxygenase. *J. Biol. Chem.* **253**, 4700-4706 (1978).
22 Freewan, M. *et al.* Human indoleamine 2,3-dioxygenase is a catalyst of physiological heme peroxidase reactions: implications for the inhibition of dioxygenase activity by hydrogen peroxide. *J. Biol. Chem.* **288**, 1548-1567 (2013).
23 Prendergast, G. C., Malachowski, W. P., DuHadaway, J. B. & Muller, A. J. Discovery of IDO1 inhibitors: from bench to bedside. *Cancer Res.* **77**, 6795-6811 (2017).
24 Ogilby, P. R. Singlet oxygen: there is indeed something new under the sun. *Chem. Soc. Rev.* **39**, 3181-3209 (2010).
25 Thomas, S. R. *et al.* Post-translational regulation of human indoleamine 2,3-dioxygenase activity by nitric oxide. *J. Biol. Chem.* **282**, 23778-23787 (2007).
26 Iida, S., Ohkubo, Y., Yamamoto, Y. & Fujisawa, A. Parabanic acid is the singlet oxygen specific oxidation product of uric acid. *J. Clin. Biochem. Nutr.* **61**, 169-175 (2017).
27 Kanofsky, J. R. Singlet oxygen production by biological systems. *Chem. Biol. Interact.* **70**, 1-28 (1989).
28 Maghzal, G. J. *et al.* Assessment of myeloperoxidase activity by the conversion of hydroethidine to 2-chloroethidium. *J. Biol. Chem.* **259**, 5580-5595 (2014).
29 Fu, R. *et al.* Enzyme reactivation by hydrogen peroxide in heme-based tryptophan dioxygenase. *J. Biol. Chem.* **286**, 26541-26554 (2011).
30 Headlam, H. A. & Davies, M. J. Beta-scission of side-chain alkoxyl radicals on peptides and proteins results in the loss of side-chains as aldehydes and ketones. *Free Radic. Biol. Med.* **32**, 1171-1184 (2002).
31 Mason, R. P. Using anti-5,5-dimethyl-1-pyrroline N-oxide (anti-DMPO) to detect protein radicals in time and space with immuno-spin trapping. *Free Radic. Biol. Med.* **36**, 1214-1223 (2004).
32 Russell, G. A. Deuterium-isotope effects in the autoxidation of aralkyl hydrocarbons. Mechanism of the interaction of peroxy radicals. *J. Am. Chem. Soc.* **79**, 3871-3877 (1957).
33 Burgoyne, J. R. *et al.* Cysteine redox sensor in PKGIα enables oxidant-induced activation. *Science* **317**, 1393-1397 (2007).
34 Headlam, H. A., Gracanin, M., Rodgers, K. J. & Davies, M. J. Inhibition of cathepsins and related proteases by amino acid, peptide, and protein hydroperoxides. *Free Radic. Biol. Med.* **40**, 1539-1548 (2006).
35 Prysyazhna, O., Rudyk, O. & Eaton, P. Single atom substitution in mouse protein kinase G eliminates oxidant sensing to cause hypertension. *Nat. Med.* **18**, 286-290 (2012).
36 Changsirivathanathamrong, D. *et al.* Tryptophan metabolism to kynurenine is a potential novel contributor to hypotension in human sepsis. *Crit. Care Med.* **39**, 2678-2683 (2011).
37 Matoba, T. *et al.* Hydrogen peroxide is an endothelium-derived hyperpolarizing factor in mice. *J. Clin. Invest.* **106**, 1521-1530 (2000).
38 Nakamura, T. *et al.* Prevention of PKG1a oxidation augments cardioprotection in the stressed heart. *J. Clin. Invest.* **125**, 2468-2472 (2015).
39 Rudyk, O. *et al.* Protein kinase G oxidation is a major cause of injury during sepsis. *Proc. Natl. Acad. Sci. U. S. A.* **110**, 9909-9913 (2013).
40 Weishaupt, K. R., Gomer, C. J. & Dougherty, T. J. Identification of singlet oxygen as the cytotoxic agent in photoinactivation of a murine tumor. *Cancer Res.* **36**, 2326-2329 (1976).
41 Munn, D. H. & Mellor, A. L. IDO in the tumor microenvironment: inflammation, counter-regulation, and tolerance. *Trends Immunol.* **37**, 193-207 (2016).
42 Cheong, J. E. & Sun, L. Targeting the IDO1/TDO2-KYN-AhR pathway for cancer immunotherapy - challenges and opportunities. *Trends Pharmacol. Sci.* **39**, 307-325 (2018).
43 Lewis-Ballester, A. *et al.* Structural insights into substrate and inhibitor binding sites in human indoleamine 2,3-dioxygenase 1. *Nat. Commun.* **8**, 1693 (2017).

Acknowledgements: We thank Dr D. Cheng, Dr S. Kong, Mr D. Newington and Mr J Wu for their technical assistance in the project, Drs N Smith and RM Graham for advice on the TAC experiments, and Drs RM Graham and CC Winterbourn for their critique on our manuscript. This work was funded by grants from the National Health and Medical Research Council of Australia (NHMRC); 1020400 to RS and RJP, and 1052616 to RS. PDM thanks FAPESP (Fundação de Amparo à Pesquisa do Estado de São Paulo, N°. 2012/12663-1, CEPID Redoxoma N°. 2013/07937-8), CNPq (Conselho Nacional para o Desenvolvimento Científico e Tecnológico, N°. 301307/2013-0), PRPUSP (Pró-Reitoria de Pesquisa da Universidade de São Paulo, NAP Redoxoma N°. 2011.1.9352.1.8) and John Simon Guggenheim Memorial Foundation (P.D.M. Fellowship) for financial support. RS is supported by a Senior Principal Research Fellowship 1111632 from the NHMRC. The work also received support from New South Wales Health.

Author contributions: G.J.M., C.P.S. and R.S. designed the study. G.J.M., A.M.G., Y.Y., R.J.P. and R.S. designed the chemical synthesis and characterization studies of *cis*-WOOH. N.N., J.O.O. and J.B.B. designed the chemical synthesis and characterization studies of epacadostat. A.M.G. and C.S. designed and carried out the purification of *cis*-norbixin. G.J.M., P.D.M., A.A. and R.S. designed the $^{1}O_2$ detection experiments. C.P.S., G.J.M., A.A., J.T., P.E. and R.S. designed the studies with isolated enzymes. C.P.S., P.C., O.P., J-P.S., Y.W., L.L.D. and R.S. designed and carried out the arterial relaxation studies. G.J.M., A.M.G., C.S., N.N., J.O.O., J.B.B. and S.S. carried out and analyzed the chemical characterization experiments. G.J.M., A.A., S.S., F.M.P. and P.D.M. carried out and analyzed the $^{1}O_2$ detection experiments. G.J.M. carried out and analyzed the *cis*-WOOH and H_2O_2 detection experiments. G.J.M., A.A., J.T., S.S., O.P. and J.S. carried out and analyzed the isolated enzyme experiments. C.P.S. and K.W. carried and analyzed arterial PKG1α experiments. K.W. designed and carried out the vascular smooth muscle studies. C.P.S. and Y.W. carried out and analyzed blood pressure experiments. Y.W., C.P.S. and R.S. designed the TAC and atherosclerosis studies. C.P.S., Y.W. and L.L.D. carried the TAC and atherosclerosis studies. All authors interpreted the data. C.P.S., G.J.M. and R.S. wrote the original manuscript and R.S. wrote the revised manuscript. All authors reviewed the revised manuscript.

Competing interests: Authors declare no competing interests

Materials & Correspondence: To be addressed to R.S

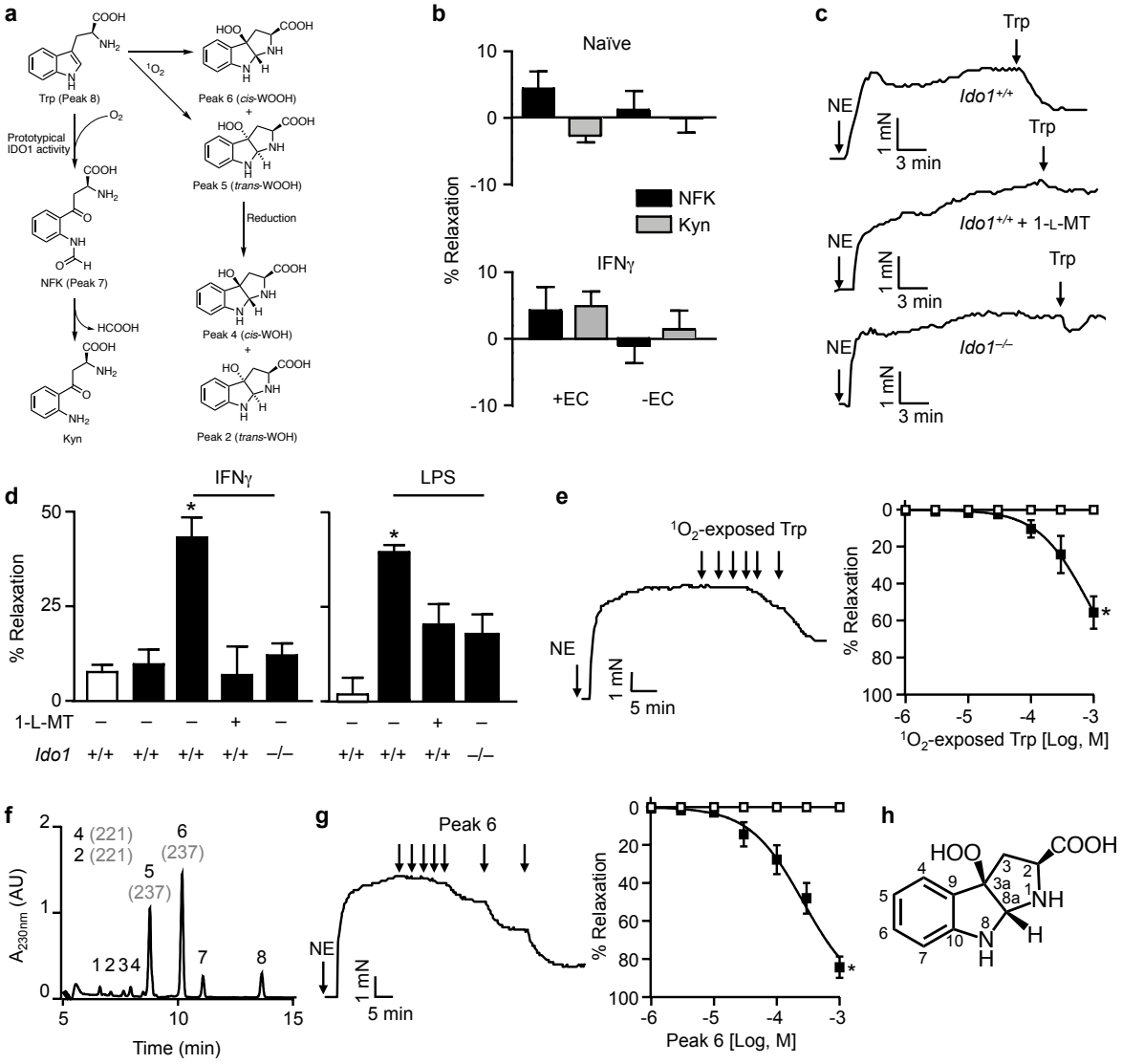

Figure 1. Identification of a tryptophan-derived tricyclic hydroperoxide as an arterial relaxant. a, Schematic of oxidation of L-tryptophan (Trp) by IDO1 (left) and $^1O_2$ (right). **b**, Relaxation of pre-constricted abdominal aortas from wildtype mice without (naïve) and with interferon-γ (IFNγ) pretreatment, and with intact (+EC) or denuded endothelium (-EC), in response to purified Kyn (n=9) or *N*-formylkynurenine (NFK) (n=4). **c**, Representative myography traces of purified Trp-induced relaxation of IFNγ-pretreated abdominal arteries from: wildtype (*Ido1*$^{+/+}$) mice without (top) and with the IDO1 inhibitor 1-L-methyltryptophan (1-L-MT) (middle); and *Ido1*$^{-/-}$ mice (bottom). **d**, Relaxation of pre-constricted abdominal aortas from *Ido1*$^{+/+}$ or *Ido1*$^{-/-}$ (n=6) mice in response to vehicle (open bars, n=18) or purified Trp (filled bars) ± 1-L-MT (n=5), with IDO1 expression induced *ex vivo* by IFNγ-pretreatment or *in vivo* by lipopolysaccharide (LPS) treatment of mice. **e**, **g**, Relaxation of pre-constricted endothelium-denuded naïve abdominal aortas to increasing amounts of $^1O_2$-exposed Trp containing all compounds present in the crude reaction mixture (**e**, n=4) and HPLC-purified Peak 6 (**g**, n=6). **f**, Typical HPLC chromatogram of the crude reaction mixture obtained after $^1O_2$ oxidation of Trp for 9 h (n=6), with numbers in bracket referring to the molecular mass of the compounds eluting as peaks 2, 4, 5 and 6. **h**, Chemical structure of Peak 6 – *cis*-WOOH. Data in **b**, **d**, **e**, and **g** are mean ± s.e.m. *p≤0.05 compared with other treatments using Kruskal-Wallis with Dunn's post hoc test (**d**) and vehicle (**e**, **g**). AU, arbitrary units; NE, norepinephrine.

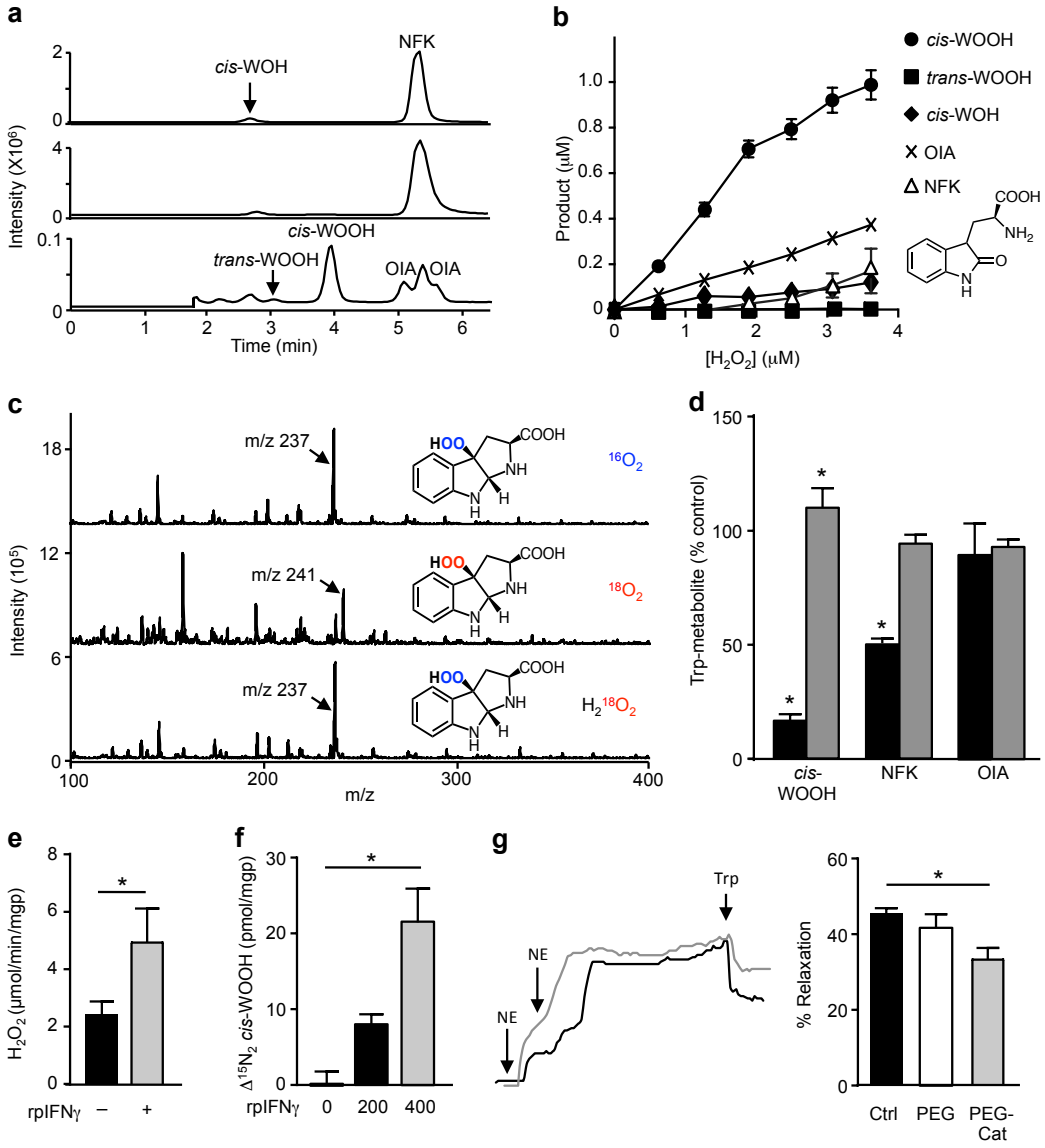

Figure 2. Arterial formation of *cis*-WOOH via oxidative activation of IDO1 dioxygenase activity. a, Total LC-MS/MS ion chromatogram of reaction mixtures of recombinant IDO1 and Trp under reducing (top, middle) and oxidizing conditions (bottom). **b**, **d**, IDO1-mediated formation of Trp-derived metabolites with successive (**b**) or bolus addition of H_2O_2 (**d**) in O_2- (grey bars) or Ar-flushed buffer (black bars). Metabolite yield is expressed as percentage of that observed in the reaction under air (**d**). The chemical structure of the peroxidase product, oxyindolylalanine (OIA), is shown in (**b**, right bottom). **c**, Full mass spectra of *cis*-WOOH derived from the reaction of IDO1 and H_2O_2 with Trp in $^{16}O_2$ (top, bottom) or $^{18}O_2$ air (middle), with H_2O_2 being replaced with $H_2{}^{18}O_2$ (bottom). **e**, Endogenous formation of H_2O_2 by porcine arteries in the absence (–) and presence of 400 ng mL^{-1} recombinant porcine interferon-γ (rpIFNγ) (+). **f**, Endogenous formation of $^{15}N_2$ *cis*-WOOH from $^{15}N_2$ L-Trp by porcine arteries pretreated with 0, 200 or 400 ng mL^{-1} rpIFNγ. **g**, Trp-induced relaxation of mouse abdominal aortas pretreated with mouse recombinant IFNγ and vehicle (black, Ctrl), polyethylene glycol (white, PEG) or PEG-catalase (grey, PEG-cat). Data are representative of 3 independent experiments (**a**, **c**) or mean ± s.e.m. of 3 (**b**, **d**, **f**), 5 (**e**) and 6 (**g**) independent experiments. *$p \leq 0.05$ compared with reaction performed under air (**d**) or for comparisons indicated (**e**, **f**, **g**), using Mann-Whitney rank sum test (**d**, **e**) or Kruskal-Wallis with Dunn's post test (**f**, **g**). $O_2^{\bullet-}$, superoxide; *cis*-WOH, hydroxide of *cis*-WOOH; cytb_5, cytochrome b_5; m/z, mass to charge ratio.

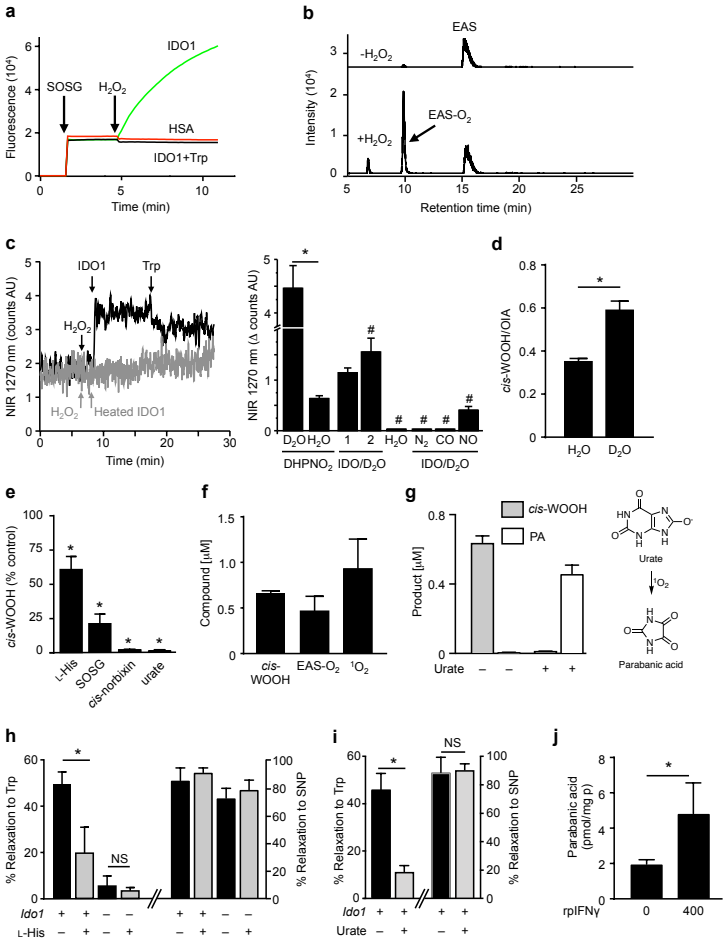

Figure 3. **Generation of $^1O_2$ by IDO1 and H_2O_2 is required for formation of *cis*-WOOH and arterial relaxation**. **a**, Fluorescence changes upon addition of H_2O_2 to Singlet Oxygen Sensor Green (SOSG) in the presence of human serum albumin (HSA, red), or IDO1 without (green) and with Trp (black). **b**, LC-MS/MS chromatograms of the reaction mixture of IDO1 and anthracene-9,10-diyldiethane-2,1-diyl disulfate disodium salt (EAS) after incubation without (top) and with H_2O_2 (bottom). **c**, Near infrared (NIR) emission upon addition of enzymatically active (black) or heat-inactivated (grey) IDO1 to H_2O_2 before and after Trp addition (left). Difference in NIR emission induced under different experimental conditions (right): 1 **d**, IDO1/H_2O_2-mediated conversion of Trp to *cis*-WOOH in phosphate buffer containing H_2O or D_2O with data expressed as a ratio of *cis*-WOOH/oxyindolylalanine (OIA). **e**, Formation of *cis*-WOOH by IDO1/H_2O_2 ± the $^1O_2$ scavenger L-histidine (L-His), Singlet Oxygen Sensor Green (SOSG), *cis*-norbixin and urate, with data expressed as yield relative to that in the absence of $^1O_2$ scavenger (control). **f**, Estimation of the $^1O_2$ generated by IDO1/H_2O_2 by quantifying the conversion of EAS to EAS-O_2. **g**, Quantification of IDO1/H_2O_2-mediated conversion of Trp to *cis*-WOOH, and urate to parabanic acid, in the absence (–) and presence of urate (+). **h**, **i** Relaxation of mouse abdominal aortas pretreated with interferon-γ ± L-His (**h**), urate (**i**) or vehicle in response to Trp or sodium nitroprusside (SNP). **j**, Formation of parabanic acid by porcine coronary arteries pretreated with 0 or 400 ng mL^{-1} recombinant porcine interferon-γ (rpIFNγ) for 51 h and 8 h in MOPS buffer prior to addition of urate. Data are representative of 3 (**a**), 2 (**b**) and 3 (**c**) independent experiments. Data in **d**, **e**, **f**, **g**, **h** and **j** are mean ± s.e.m. of 3 independent experiments, while data in **i** are mean ± s.e.m. of n=7 (Trp) and n=4 (SNP) experiments. *#$p \leq 0.05$ as determined by Mann-Whitney test for comparison with standard reaction condition using 1 μM IDO1 (# in **c**) or as indicated (* in **c**, **d**, **g**). $DHPNO_2$, endoperoxide of *N*,*N*-di(2,3-dihydroxypropyl)-1,4-naphthalene dipropanamide, used as a positive control; 1, 1 μM IDO1; 2, 2 μM IDO1; N_2, reaction mixture bubbled with N_2 to remove O_2; CO and NO, IDO1 treated with CO and NO, respectively; EAS-O_2, endoperoxide of EAS.

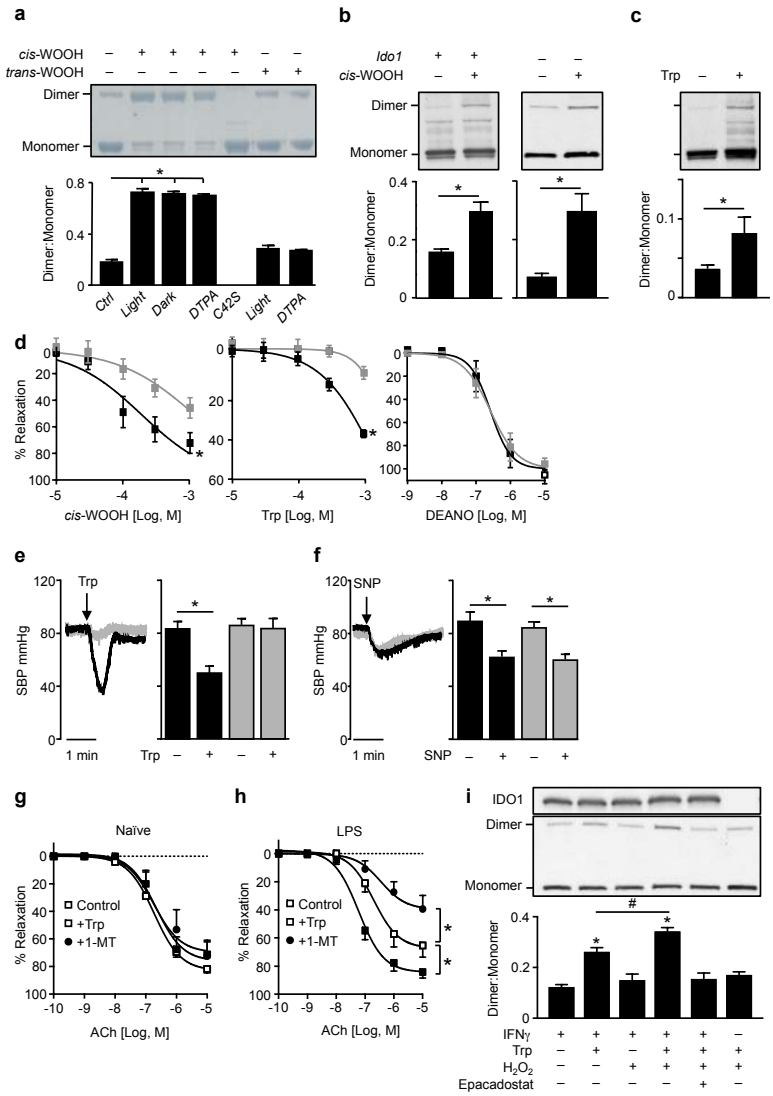

Figure 4. Regulation of arterial relaxation and blood pressure by IDO1-mediated Trp metabolism is dependent on cysteine residue 42 of PKG1α. a, Dimerization of recombinant human wildtype and cysteine 42 serine (C42S) mutant PKG1α by *cis*- and *trans*-WOOH ± light and the transition metal chelator diethylenetriaminepentaacetic acid (DTPA); n=3 separate experiments. **b**, **c**, Dimerization of PKG1α in mouse mesenteric resistance arteries by (**b**) *cis*-WOOH (left, naïve arteries from wildtype mice, n=10), (right, naïve arteries from *Ido1*$^{-/-}$ mice, n=4) or (**c**) Trp (arteries from lipopolysaccharide (LPS)-treated wildtype animals, n=4). **d**, Relaxation of pre-constricted mouse mesenteric resistance arteries from wildtype (black) and PKG1α C42S knock-in mice (grey) by *cis*-WOOH (naïve arteries, n=3 for both genotypes), or Trp (n=4 for both genotypes) and the nitric oxide donor sodium 2-(*N*, *N*-diethylamino)-diazenolate-2-oxide (DEANO) (arteries from lipopolysaccharide-treated animals, n=4 for both genotypes). **e**, **f**, Blood pressure responses elicited by Trp (**e**), sodium nitroprusside (SNP) (**f**) in endotoxemic wildtype (black, n=8 for Trp, n=4 for SNP) or PKG1α C42S knock-in mice (grey, n=9 for Trp and SNP). **g**, **h**, Acetylcholine (ACh)-induced relaxation of mouse mesenteric resistance arteries from naïve (**g**) or LPS-treated (**h**) wildtype mice in the absence (control, n=4 for naïve, n=13 for LPS) or presence of Trp (n=4 for naïve, n=10 for LPS) or 1-L-methyltryptophan (1-MT, n=4 for naïve, n=8 for LPS). **i**, Dimerization of PKG1α in human smooth muscle cells induced by Trp, 1 μM H_2O_2 or both, in the presence (+) or absence (–) of the IDO1 inhibitor epacadostat (n=5). These cells were pretreated with (+) or without (–) 100 ng mL^{-1} recombinant human interferon-γ (IFNγ) for 72 h. Data are representative or mean ± s.e.m. *$^{\#}$p≤0.05 as determined by Mann-Whitney rank sum test (**a**, **b**, **c**), 2-way ANOVA with Šidák post-hoc test (**d**), Kruskal Wallis with Dunn's test (**e**, **f**, **i**), and 1-way ANOVA of maximal relaxation values with Dunnett's test (**g**, **h**).

Extended data, figure legends

Extended data, figure 1. Only Peak 6 induces arterial relaxation in resistance and conduit arteries from different vascular beds and species. a, Concentration-dependent arterial relaxation of norepinephrine (NE) pre-constricted, endothelium-denuded mouse abdominal aorta by purified Peaks 1-6. **b-f,** Peak 6 concentration-dependent arterial relaxation in endothelium-denuded murine (**b**), rat (**c**, **d**, **e**), and porcine (**f**) arteries pre-constricted with NE (**b**, **c**) or the thromboxane A_2 receptor agonist U46619 (**d**, **e**, **f**). Data show mean ± s.e.m of n=4 (**a-e**) and n=5 (**f**) independent experiments, with diameter range of the arteries indicated.

Extended data, figure 2. Characterization of reaction products formed during $^1O_2$-mediated oxidation of tryptophan by liquid chromatography with tandem mass spectrometry (LC-MS/MS). a, Representative LC-MS chromatogram of reaction products from the oxidation of L-tryptophan by Rose Bengal/O_2/light showing molecular ions, $[M+H]^+$ for peaks 1-8, representative of n=6. **b**, Tandem mass (MS/MS) spectra of precursor ions with mass-to-charge (m/z) ratio of 221 (Peaks 2 and 4) and 237 (Peaks 5 and 6), representative of n=2 independent experiments.

Extended data, figure 3. Chemical identification of Peaks 2, 4, 5 and 6. a, HPLC chromatograms of reaction products from L-tryptophan oxidation by Rose Bengal/O_2/light showing retention times of Peaks 1-6 monitored at 230 nm and their corresponding post-column chemiluminescence (CL) signals. **b**, HPLC-UV and CL chromatograms of Peaks 5 and 6 after their chemical reduction with sodium borohydride. **c**, Comparison of molecular ions and fragmentation pattern of Peaks 2 and 4 with those of chemically reduced Peaks 5 and 6. **d**, Comparison of ^1H NMR spectra of Peaks 2 and 4 (top) with those of chemically reduced Peaks 5 and 6 (bottom). Data shown are representative of n=2 independent experiments (**a-d**).

Extended data, figure 4. Stereochemical characterization of Peaks 2 and 4. a, **b**, ^1H NMR spectra (top) of irradiated Peak 2 (**a**) in CD_3OD/D_2O and Peak 4 (**b**) in CD_3OD (top spectra). The arrow indicates the spectral peak irradiated. The bottom spectra show the respective NOE differential spectra of the irradiated peak with the dashed oval indicating anti-phase NOE interaction. Data shown are spectra from 1 experiment (**a**, **b**). **c, d,** Structures of Peak 2 (*trans*-WOH) and Peak 4 (*cis*-WOH) showing irradiated proton H_{8a} and indication of the NOE correlation.

Extended data, figure 5. Conversion of *cis*-WOOH to *N*-formylkynurenine (NFK). a, Spectral changes during incubation of *cis*-WOOH in phosphate buffer at 37 °C measured in 15 min intervals. Arrows indicate increase (↑) and left shift (←) in absorbance, while inset shows spectrum of authentic NFK. **b**, ^1H NMR spectra of *cis*-WOOH in D_2O and 25 °C recorded at 5 min (top) and 360 min (middle). Arrows indicate increases in spectral peaks at 4.1, 7.6, 7.9, 8.1 and 8.3 ppm. Bottom shows ^1H NMR spectra of authentic NFK. **c**, Time-dependent loss of *cis*-WOOH and formation of NFK during incubation of *cis*-WOOH at 37 °C in the presence of diethylenetriaminepentaacetic acid, as assessed by LC-MS/MS. **d**, Light emission upon addition of *cis*-WOOH in D_2O phosphate buffer at 72 °C, with corresponding chemiluminescence spectra. **e**, Proposed mechanism of formation of *cis*-WOOH from $^1O_2$-mediated oxidation of Trp. Data shown are representative spectra of 1 (**b**, **c**) and 2 separate experiments (**a**, **d**).

Extended data, figure 6. Role of $^1O_2$ in IDO1/H_2O_2-mediated oxidation of Trp to *cis*-WOOH and Trp-induced arterial relaxation. a, LC-MS/MS analysis of *cis*-WOOH (circles) and *trans*-WOOH (squares) following exposure of L-tryptophan to Rose Bengal/O_2/light for the time indicated. **b,** Formation of *cis*- and *trans*-WOOH during oxidation of Trp by Rose Bengal/O_2/light (RB) and IDO1/H_2O_2. **c**, Inhibition of IDO1/H_2O_2-mediated *cis*-WOOH formation by different pharmacological IDO1 inhibitors (all tested at 1 mM), with results expressed as the percentage of *cis*-WOOH formed in presence versus absence of inhibitor (control). **d**, Fluorescence changes upon

addition of H_2O_2 to Singlet Oxygen Sensor Green (SOSG) in the presence of either IDO1 ± inactivated carbon monoxide-releasing molecule-A1 (iCORM-A1) (green), IDO1 pre-treated with CORM-A1 (red), DEANO (black), or urate (blue). **e**) Near infrared (NIR) emission upon addition of IDO1 pre-treated with CO gas to H_2O_2. **f**, Formation of *cis*- and *trans*-WOOH during oxidation of Trp by horseradish peroxidase (HRP)/H_2O_2, myeloperoxidase (MPO)/H_2O_2 and purified IDO2/H_2O_2. **g**, Trp-induced relaxation of pre-constricted abdominal aortas from wildtype (WT), *Ido1*$^{-/-}$ or *Ido1*$^{-/-}$*Ido2*$^{-/-}$ mice. **h**, Effect of *cis*-norbixin (100 μM) on relaxation of mouse mesenteric resistance arteries induced by Trp or the nitric oxide donor sodium 2-(*N*, *N*-diethylamino)-diazenolate-2-oxide (DEANO) (arteries from lipopolysaccharide-treated animals, n=4). In **b**, **c**, and **f**, reactions were initiated by the addition of H_2O_2/Trp and the mixtures incubated for 5-15 min at 25 °C before products were quantified by LC-MS/MS. Data show mean ± s.e.m. or representative data (**d**, **e**) of 3 independent experiments. 1-MT, 1-methyltryptophan; Ep, epacadostat; NLG, NLG919.

Extended data, figure 7. Mechanism of $^1O_2$ formation by IDO1/H_2O_2. For all reactions, IDO1 (2 or 4 μM) was incubated for 5 min (**h** for 30 min) at 25 °C with 50-fold molar excess of H_2O_2 in the presence of the scavengers and substrates indicated. **a**, **b**, Effect of Cu/Zn superoxide dismutase (SOD) and *N*-ethylmaleimide (NEM) on *cis*-WOOH formation by IDO1/H_2O_2. Reactions were initiated by the addition of H_2O_2 and the mixtures (containing 100 μM diethylenetriaminepentaacetic acid and 100 μM Trp) incubated for 5 min at 25 °C before *cis*-WOOH was quantified by LC-MS/MS. Results in **a** are expressed as the percentage of *cis*-WOOH formed in the presence versus absence (control) of 100 U SOD, whereas in **b** results are expressed as percentage of Trp converted to *cis*-WOOH. **c**, Effect of IDO1/H_2O_2 on conversion of hydroethidine (HE) to 2-chloroethidium (2-Cl-E^+) in phosphate buffered saline (PBS), as determined by LC-MS/MS. **d,** Effect of scavengers of excited carbonyls (sorbate) and oxygen-centered radicals (5,5-dimethyl-1-pyrroline *N*-oxide; DMPO) on the formation of *cis*-WOOH by IDO1/H_2O_2. **e**, Formation of IDO1 fragments (double arrow) and dimers (arrow) upon reaction of IDO1 with H_2O_2 in the absence or presence of Trp or DMPO as assessed by SDS-PAGE under non-reducing conditions and visualization of proteins by silver stain. **f**, **g**, Formation of dityrosine and IDO1 hydroperoxides during exposure of IDO1 to H_2O_2 in 100 mM phosphate buffer in the absence of Trp ± DMPO (**f**) or ± ascorbate (Asc, **g**). Reaction mixtures were subjected to size exclusion chromatography with HPLC-UV_{214nm} (left) and (**f**) fluorescence or (**g**) post-column chemiluminescence (CL) detection (right). Ascorbate was used as a reductant for protein hydroperoxides. **h**, IDO1/H_2O_2-mediated conversion of EAS (1 mM) to EAS endoperoxide (EAS-O_2) in the absence and presence of DMPO. **i**, Formation of protein carbonyls during reaction of IDO1 with H_2O_2 in the absence and presence of DMPO. Following reaction, IDO1 was denatured with 6% SDS in the presence of dinitrophenylhydrazine (DNPH) before protein was transferred onto nitrocellulose membrane, and carbonyls detected using anti- DNPH antibody. Qualitative data are representative of 2-3 separate experiments. Quantitative data show mean ± s.e.m. of 3 independent experiments. *$P \leq 0.05$ (Mann-Whitney test).

Extended data, figure 8. Role of protein kinase G1α (PKG1α) in arterial relaxation by IDO1/*cis*-WOOH. a, **b** Concentration-response curves to *cis*-WOOH after pre-treatment of denuded mouse abdominal aortas with vehicle (filled squares) or the competitive cGMP PKG inhibitor RP-8CPT-cGMP (**a**, open squares), or the competitive ATP binding PKG inhibitor KT5283 (**b**, open squares). **c**, **d**, IDO activity in kidney homogenate (**c**) or plasma (**d**) obtained from wildtype (WT) or PKG1α C42S knock-in (KI) mice after treatment with lipopolysaccharide. Data show mean ± s.e.m. of 5 (**a**), 4 (**b**, **c**) or 6 (**d**) independent experiments. *$p \leq 0.05$ using repeated measures 2-way ANOVA with Šidák multiple comparison post-hoc test. NS, not significant (Mann-Whitney test).

Extended data, figure 9. Role of IDO1 in pressure-overload related cardiac pathophysiology and experimental atherosclerosis. a, Cardiac expression of Ido1 mRNA after sham and transverse

aortic constriction (TAC) for 21 days, with IFNγ-treated hearts as positive control. Inset: increase in ventricle weight-to-tibia length ratio as evidence for TAC-induced cardiac hypertrophy. **b**, **c**, IDO1 staining (brown color) in (**b**) atherosclerotic lesions of thoracic aorta and (**c**) resistance vessel of kidney of *Apoe*$^{-/-}$ (top) and *Apoe*$^{-/-}$*Ido1*$^{-/-}$ (middle) mice after six months of Western Diet (WD), with isotype rabbit IgG as control (bottom). Magnification 60x (**b**) and 20x (**c**). Arrow heads (**c**) indicate microvessels. **d**, Plasma concentrations of L-tryptophan (Trp) and kynurenine (Kyn) in *Apoe*$^{-/-}$ and *Apoe*$^{-/-}$*Ido1*$^{-/-}$ mice after six months of WD. **e**, Trp-induced relaxation of pre-constricted, atherosclerotic lesion-containing aortic rings isolated from *Apoe*$^{-/-}$ and *Apoe*$^{-/-}$*Ido1*$^{-/-}$ mice in the presence or absence of IDO1 inhibitor 1-methyltryptophan (1-MT) after six months of WD. **f**, Systolic blood pressure (SBP) of *Apoe*$^{-/-}$ and *Apoe*$^{-/-}$*Ido1*$^{-/-}$ mice before (–) and after (+) administration of 1-D-MT. n, number of mice used. *$p \leq 0.05$ (Mann-Whitney test).

Extended data, table 1. ^{1}H and ^{13}C NMR data for purified Peaks 2, 4, 5 and 6 in D_2O (calibrated to 4.79 ppm)

Extended data, scheme 1. Proposed mechanism for formation of $^{1}O_2$ by IDO1 plus H_2O_2. Reaction of Fe^{3+}-heme IDO1 with H_2O_2 results in formation of the two-electron oxidized form, compound I, consisting of a Fe^{4+}=O iron center and a porphyrin cation radical (not shown). The latter is transferred to an amino acid side chain of IDO1, such as Trp (not shown) or, more likely, Tyr such as Y126 or Y353 that are close to the active site heme in IDO1[43]. The IDO1 tyrosyl radical may then engage in the formation of fluorescent di-tyrosine crosslinks or H-abstraction reactions leading to protein fragmentation according to established pathways[30]. Alternatively, a resonance form of the IDO1 tyrosyl radical may add to molecular oxygen. The resulting intermediate quinone peroxyl radical may then participate in inter- or intra-residue peroxyl radical combination, the latter subsequent to additional H-abstraction and oxidation reactions and formation of a putative intra-residue di-peroxyl radical. The resulting tetroxides will decay with release of $^{1}O_2$ according to the Russell Mechanism[32]. The observed stereospecific formation of *cis*-WOOH by IDO1/H_2O_2/L-Trp suggests formation of $^{1}O_2$ close to the active site heme rather than release into the bulk phase, and may therefore be more consistent with the intra-residue peroxyl radical combination pathway.

Extended data, scheme 2. Chemical synthesis of epacadostat.